CHAPTER IV
RHEOLOGICAL, MORPHOLOGICAL, THERMAL, AND MECHANICAL PROPERTIES OF BLENDS OF VECTRA A950 AND POLY(TRIMETHYLENE TEREPHTHALATE): A STUDY ON A HIGH-VISCOSITY RATIO SYSTEM

4.1 Abstract

Poly(trimethylene terephthalate) (PTT) and a liquid crystalline polymer, Vectra A950 (VA), were melt-blended and subjected to capillary rheometry. Effects of VA content, shear rate, and temperature on viscosity and flow activation energy (E_a) were investigated. Partial fibrillation was found even though the viscosity ratio was greater than one, leading to the formation of in-situ composites. Thermal and thermogravimetric analysis of the blends suggested that they were immiscible and their thermal stabilities were enhanced. From tensile tests, the incorporation of VA improved tensile modulus, slightly decreased tensile strength, and drastically lowered elongation at break, compared to neat PTT. It was found that the blend with the best VA dispersion can be achieved at the minimum VA content (10 wt%) and lowest processing temperature (250°C). Not only did this blend exhibit improved mechanical properties comparable to those of blends processed at temperatures closer to the crystalline-to-nematic transition of VA (~280°C), it also shows enhanced processibility through the reduction of both melt-viscosity and E_a.

Key words: In-Situ Composites; Liquid Crystalline Polymer; Mechanical Properties; Rheology; Thermal Properties

4.2 Introduction

Liquid crystalline polymers (LCPs) are remarkably high performance thermoplastics known to exhibit high modulus, high strength, high toughness, good creep resistance, and low coefficients of thermal expansion. The unique features of these polymers are their low shear viscosity in the nematic molten state and their high molecular alignment in the solid state after thermoplastic processing. These distinctive properties arise from their stiff linear molecular structure, which makes them readily align to the flow direction. The incorporation of an LCP as a minor phase into a typical thermoplastic may offer the potential of improved melt processibility. In addition, due to the intrinsically high modulus of an LCP phase, the mechanical properties of the blends could be enhanced.

Although much effort has been put into blends of an LCP with a terephthalate-based ester, like poly(ethylene terephthalate) (PET) or poly(butylene terephthalate) (PBT) [1-4], blends of an LCP with a recently-commercialized terephthalate-based polyester, namely poly(trimethylene terephthalate) (PTT), to the best of our knowledge, have not yet been investigated. Due to the similarity in their chemical structures, PTT has an unusual combination of the outstanding properties of PET and the processing characteristics of PBT, giving rise to its potential as a thermoplastic for carpeting, textiles, film, packaging, and engineering thermoplastic applications. The introduction of LCP, which possesses high mechanical properties, might be able to improve the tensile properties of the PTT required for certain engineered thermoplastic applications.

According to statistical thermodynamic analysis, perfectly rigid rod LCPs are immiscible with flexible coil polymers, giving rise to a separated LCP phase [5]. As a matter of fact, it has been reported that under certain flow conditions and with an appropriate range of LCP concentration, the LCP domains can elongate into fine fibrils and reinforce the matrix. Thus, these blends are commonly referred to as in-situ composites [6]. In-situ composites are considered to be competitive with glass fiber-reinforced composites where processibility and low density are dominant requirements.

The final properties of in-situ composites depend on their phase morphology, which is affected by several important factors. These are, for example, LCP content, processing conditions, viscosity ratio (disperse phase to matrix phase), and the interfacial adhesion. Processing conditions, including temperature, and shear and extensional forces, strongly affect the molecular orientation of the LCP phase as well as the LCP fibril aspect ratio. Among these parameters, a viscosity ratio near or less than unity has been reported necessary for LCP fibrillation. However, some researchers claimed that for certain LCP/thermoplastic pairs, the fibrillation can occur at a viscosity ratio much higher or lower than unity [7,8]. Beery et al. [9] indicated that, as well as the viscosity ratio, interfacial forces between the thermoplastic matrix and LCP domains are major parameters that control the development of fibrils. This leads to the contradictory results on the effect of viscosity ratio on the fibrillation for different blend systems. The combined effects of viscosity, interfacial tension, and shear rate may be represented by the capillary number, Ca, expressed as:

$$Ca = \frac{\eta_m \dot{\gamma}}{\sigma / R} \qquad (4.1)$$

where η_m is the matrix viscosity, $\dot{\gamma}$ the shear rate, R the LCP droplet radius ($R = D/2$), and σ the interfacial tension of polymer pairs. According to Taylor [10,11], the capillary number is the ratio of the two opposing forces, i.e. the viscous forces that tend to deform the droplet to the counteracting interfacial forces that tend to resist the deformation and keep the droplet shape spherical. To achieve a fibrillar morphology, a high degree of deformation will be required. In other words, the higher the capillary number, the easier the droplet deformation. From the above equation, the shear stress ($\eta_m \dot{\gamma}$) should be larger than half of the interfacial energy (σ / D) but lower than the melt strength of the LCP to achieve LCP fibrils. The simplest way to increase the shear stress could be by lowering the processing temperatures, which in turn enhances the matrix viscosity. This should be a suitable method for a system in which the viscosity of the matrix is more sensitive to temperature than that of the LCP. There are a number of

research works dealing with processing conditions—structure/mechanical property correlations. For blends of an LCP with a thermoplastic like PBT or Nylon6, Beery and co-workers [9] reported improvements in the tensile properties with decreasing extrusion temperature. Bastida *et al.* [12] observed the reverse manner in injection molded blends of poly(ether imide) and a thermotropic copolyester, Rodrun LC-5000. Mostly, the processing temperature could be manipulated to provide sufficient viscous force able to elongate the LCP domains for a specific polymer pair. Recently, Kalkar *et al.* [13], as well as Tan *et al.* [14], carrried out systematic studies on the effect of temperature on the viscosity ratio and the resulting tensile properties. However, their study was done on a system with a viscosity ratio close to unity; hence, further study under higher viscosity ratio conditions should be performed.

In the present contribution, the rheological, morphological, thermal, and mechanical properties of blends of Vectra A950 (VA)/PTT were investigated. It should be noted that this system was a high viscosity ratio system where the viscosity of PTT is much lower than that of VA. The flow behavior of the VA/PTT binary blends at different temperatures, shear rates, and LCP contents was studied using a capillary rheometer. The morphology of the rheometer extrudates, observed by scanning electron microscope (SEM), was related to the rheological results. Studies on the thermal characteristics of the blends by means of differential scanning calorimetry (DSC) and thermogravimetric analysis (TGA) were also conducted. Tensile testing was performed on the injection-molded specimens.

4.3 Experimental

4.3.1 Materials

Poly(trimethylene terephthalate) (PTT) was kindly supplied in pellet form by PTT PolyCanada LP (Corterra 9200). Its intrinsic viscosity (IV) is 0.92 dl/g. The LCP used was Vectra A950 (labeled VA hereafter), supplied by Hoechst-Celanese. VA is a copolyester of 73 mol% p-hydroxybenzoic acid (HBA) and 27 mol% 2-hydroxy-6-

naphthoic acid (HNA). All the materials were dried in a vacuum oven at 130°C for at least 12 h prior to use.

4.3.2 Preparation of Blends

PTT and VA resins were premixed in a dry mixer to prepare VA/PTT blends with VA contents of 10, 20, 30, 40, 50, and 70 wt%. The samples were designated as VA wt%; for example, a blend containing 10 wt% VA and 90 wt% PTT would be represented as VA10. The dry-mixed blends were melt-mixed in a self-wiping, co-rotating twin-screw extruder (Collin, ZX-25). The temperature of the barrel section from the feeding zone to the die was set at 80, 230, 250, 275, 285, and 265°C. The rotor was operated at a speed of 30 rpm. The extrudates were cooled by water and then pelletized.

The neat PTT and VA10 pellets were dried and injected into dumbbell-shaped specimens 2.5 mm thick on an AP-90 (Asian Plastic) injection molding machine for the tensile tests. (The injection molding conditions are provided in Table 4.1.)

4.3.3 Rheological Measurement

A CEAST Rheologic 5000 twin-bore capillary rheometer was used to measure the shear viscosity of the blends. The inner diameter and the length of the barrel used were 15 and 250 mm, respectively, while the inner diameter and the length of the die were 1 and 20 mm (i.e. L/D ratio = 20), respectively. The temperature tolerance was set at ±0.5°C. An automatic data collection system was used to analyze the test results. The apparent shear viscosity of the blends in the temperature range of 250–280°C and a shear rate range of 60–2000 s^{-1} was recorded. The rheometer extrudates were quenched at room temperature and collected for further SEM analysis.

4.3.4 Morphological Observation

The morphology of the blends was observed using a JEOL JSM5200 scanning electron microscope (SEM). The specimens were cryogenically fractured in

liquid nitrogen in the transverse direction to provide a cross-sectional view. The rheometer extrudates were also immersed in 1,2-dichlorophenol at 80°C for 2 h to dissolve the PTT matrix as the first step, followed by repeated washing of the residue for a clear LCP phase. The fractured surfaces and the LCP residue were sputtered with a thin layer of gold prior to observation

4.3.5 DSC Characterization

The differential scanning calorimeter measurements were carried out by using a Mettler-Toledo DSC822 differential scanning calorimeter (DSC). All measurements were performed under a dry nitrogen atmosphere. The instrument was calibrated in both the temperature and the melting enthalpy with a standard sample of indium to ensure the accuracy and reliability of the data. To avoid an uneven thermal conduction of the samples, each sample holder was loaded with samples of comparable quantity (8±0.5 mg).

The experiments started with heating PTT, VA, and their blends obtained from the twin-screw extruder from 25°C to a fusion temperature of 300°C at a heating rate of 200°C min^{-1} for a melt-annealing period of 5 min in order to remove previous thermal histories, after which the samples were removed and immediately quenched in liquid nitrogen to achieve a completely amorphous state of the samples. The quenched sample was immediately subjected to a heating scan at a rate of 5°C/min from 25°C to 300°C. The sample was then cooled to 30°C at a cooling rate of 10°C min^{-1}. The second heating and cooling traces were recorded.

4.3.6 Thermogravimetric Analysis

The thermal stability of PTT, VA, and their blends from the twin-screw extruder was evaluated by a Perkin Elmer TGA7 (TGA) operated under nitrogen atmosphere at a heating rate of 10°C min-1 from 30 to 800°C. Decomposition temperature and the weight percent of the residue were recorded.

4.3.7 Static Mechanical Preoperties

Tensile tests were conducted in an Instron 4206 tensile tester at room temperature. The mechanical properties (tensile modulus, tensile strength, and elongation at break) were determined from the stress–strain curves. At least seven specimens were tested for each reported value.

4.4 Results and Discussion

4.4.1 Rheological Behavior

The plots of viscosity versus shear rate for the neat components and the blends at various compositions and temperatures are presented in Fig. 4.1. All specimens exhibit shear thinning behavior; i.e., the viscosity decreases with increasing shear rate due to the induced chain orientation, resulting in a lower entanglement density [15]. Apparently, the neat VA displays greater shear-thinning over the whole shear rate range than the neat PTT. From Figs. 4.1(a) and 1(b), the neat PTT shows relatively low viscosity, less than 100 Pa.s and it seems to reach its Newtonian regime at temperatures higher than 270°C or shear rate greater than 100 s^{-1}. The Newtonian regime indicates that the PTT chains become nearly fully disentangled. Interestingly, introducing VA into the system could enhance its shear-thinning behavior. It can be seen that the viscosity curves of VA20 and VA30 (the blends with VA 20 wt% and 30 wt%, respectively) intersect. Intersecting viscosity curves have been found before in other systems of liquid crystalline polymer/thermoplastic blends [16,17]. It is important to note that only at 250°C and 260°C [Figs. 4.1(c) and (d)], VA10 exhibits the viscosity reduction phenomenon compared to the matrix viscosity. Generally, this viscosity reduction phenomenon has been ascribed to the deformation of the LCP phase into fibrils and the orientation of these deformed fibrils in the direction of flow. Another possible reason could be the interfacial slip between VA and the thermoplastic matrix due to the lack of adhesion [4,18]. Both reasons originate from the incompatibility of the LCP and the thermoplastic matrix. VA chains are usually rigid and stiff, while PTT chains are much

more flexible. Mixing the LCP with the flexible-coil polymer mostly results in the positive free energy of mixing and, as a consequence, phase separation occurs. With the further SEM analysis of extrudates of various extrusion temperatures, shear rate, and VA contents, we could establish the relationship between the change in the blend viscosity and the final phase morphology (see the Morphology of the Rheometer Extrudate section).

When the viscosity is plotted semi-logarithmically against the blend composition, it is observed that the viscosity increases with increasing VA content [Fig. 4.2], except for VA10 at 250°C and 260°C where a reduction in blend viscosity occurs as stated earlier. Starting from the highest temperature (280°C), the viscosity of VA10 is obviously greater than that of the neat PTT; and at a temperature of 270°C, its viscosity is just above that of the neat PTT. At 260°C and 250°C, VA10 exhibits viscosity reduction, compared to that of PTT. The extent of reduction also varies depending on the temperature; i.e. at 250°C, the reduction in viscosity is more pronounced than at 260°C. The source of these differences will be discussed later in the morphology section.

As mentioned earlier, it has been reported that fibrillation is mostly achieved when the viscosity of LCP is lower than that of the matrix. In other words, a viscosity ratio near or smaller than unity favors the fibrillation of LCP [19]. The data shown in Fig. 4.3 indicate that the viscosity ratio decreases with increasing shear rate and decreasing temperature. Therefore, it could be expected that the fibrillation of LCP would be enhanced at higher shear rate and lower temperature as well. However, all viscosity ratio values are still far higher than unity. Based on the viscosity ratio criterion alone, under these flowing conditions, it might be difficult to obtain any LCP fibrils. It will be shown in the morphology section that under proper flow conditions and VA content, fine fibrils, along with spherical domains, could be observed. Hence, LCP fibrillation does not entirely depend on the viscosity ratio. In this case, at high viscosity ratio and high temperature, LCP domains were deformed into fibrils, which were rarely broken into small droplets due to the low-viscosity, Newtonian-like matrix. By reducing the temperature, the PTT matrix becomes more viscous and thus can exert greater shear

force to deform the dispersed VA phase. For other temperatures of investigation that are below 280°C (a crystalline-to-nematic transition temperature of VA), VA can still undergo deformation, as evidenced in the morphology section. Due to the higher shear stress acting upon the VA domains at lower temperature or higher shear rate, the VA fibrils can be broken down further into small spherical droplets as these fibrils suffer from capillary instability. In other words, the capillary number is increased with lowering temperature or increasing shear rate. Due to the immiscibility, both fine fibrils and small soft droplets with a partly nematic structure act as a lubricant that can reduce the viscosity of the matrix by gliding the matrix polymeric chains to the direction of flow.

Adjusting the fabrication temperature could be an effective way to enhance LCP fibrillation (as well as improve mixing), especially for a system in which the matrix is more sensitive to temperature than LCP. Thus, it is interesting to investigate the temperature dependence of the shear viscosity employing the so-called Arrhenius–Eyring equation [20]:

$$\eta_a = A_0 \exp\left(\frac{E_a}{RT}\right) \qquad (4.2)$$

where η_a is the melt viscosity at temperature T, R the universal gas constant, A_0 a frequency term depending on the entropy of activation for flow, and E_a is taken to be the activation energy for viscous flow. A linear correlation was found in the plot of $ln\eta_a$ vs. $1/T$ of all the samples [Fig. 4.4], which has proven that the Arrhenius–Eyring equation is applicable to these binary VA/PTT blends. The value of E_a can be obtained from the linear regression of $ln\eta_a$ vs. $1/T$ at different shear rates. After calculation, the E_a values expressed in kJ/mol were plotted against the VA content, as displayed in Fig. 4.5.

The flow activation energy can be used to represent the sensitivity of a polymer to temperature; that is, the higher the E_a, the higher the sensitivity. Normally, the viscosity of a polymer is less sensitive to temperature at higher shear rate; i.e., the E_a becomes smaller as shear rate increases. This is attributed to the greater destruction of the coupling point of the entanglement network under high shear, and hence results in a

decrease of interaction between chain segments. From Fig. 4.5, VA and PTT show smaller E_a values at higher shear rate, as expected for typical polymers. PTT behaves twice as temperature sensitive as VA and thus leads to the smaller viscosity ratio at low temperature. The low temperature sensitivity of VA infers its stiff molecular structure and low entanglement density that make its flow properties less affected by temperature change. The blends show E_a values between that of PTT and VA. The addition of VA leads to a drastic drop in E_a at first (10 wt% VA), then it increases to the maximum at 50 wt% VA, and falls again at 70 wt% VA. Hence, a greater VA content is less effective in the disruption of the polymeric chain entanglement. The fall of E_a at 70 wt% VA can be expected since at this composition, the PTT becomes the minor phase. With increasing shear rate, the maximum E_a tends to shift to blends with lower VA content.

4.4.2 Morphology of the Rheometer Extrudates

The SEM micrographs of the lateral cross sections of the VA/PTT blends collected from the extruder and from the rheometer are shown in Figs. 4.6(a) and (b), respectively. All of the samples clearly reveal a biphasic morphology typical of highly immiscible blends. For the samples collected from the extruder, the shape of the VA domains is mainly spherical [Fig. 4.6(a)]. However, as shown in Fig. 4.6(b), the morphology of the rheometer extrudate shows both spherical and fibrillar domains, indicating the influence of processing conditions on the final morphology of the blends.

It has been discussed that a high capillary number promotes deformation. One could increase the capillary number by increasing the shear stress exerted on the LCP domains. This could be achieved by either lowering the temperature or increasing the shear rate. From the cross-sectional view of the rheometer extrudate at the high extrusion temperature of 260°C and a shear rate of 2000 s^{-1} [Figs.4.7 (a)–(f)], the dispersed VA phase first appears at low content as fibrillar and spherical domains, and the domains become bigger with increasing VA content due to the phase coalescence [16,21]. It is found that even when VA is the major phase (VA70), instead of the VA becoming the matrix, it forms thick, continuous fibrils surrounded by the PTT phase.

This is because the PTT phase is much less viscous than the VA phase. In general, the component with lower viscosity will tend to encapsulate the more viscous component, since this decreases the rate of energy dissipation by mixing. The larger size of the VA domains obtained at higher VA content leads to lowered interfacial area and interfacial slippage. Thus, a rise in blend viscosity is observed with increasing VA content. To clearly depict the influence of extrusion temperature on the blend morphology, the PTT phase was etched out from VA10 samples of various extrusion temperatures [Figs. 4.8(a)–(d)]. All the samples reveal both spherical and fibrillar VA domains, but at different sizes and proportions. It is worth noting that even though the viscosity ratio is higher than one for all cases, partial fibrillation is still observed. At high temperature, low shear stress applied by the nearly-Newtonian PTT matrix yields larger fibrils and beads. By lowering the temperature, the imposed shear stress becomes stronger and enough to cause intense fibrillation and droplet break-up. Therefore, a number of small spherical domains and fine fibrils of a few microns thick are found at 250 and 260°C. This implies that at low temperature, a small viscosity difference leads to improved mixing, but we might lose the fibrillated domains to break-up as these domains suffer capillary instability at such high shear stress. Due to the broad distribution in sizes of both VA fibrils and beads, it is more informative to provide morphological data in terms of VA diameter instead of VA aspect ratio. According to Fig. 4.9, finely-dispersed VA domains (mostly obtained at low temperature) are strong evidence for enhanced mixing. The higher the temperature is, the more the major population shifts towards larger diameter. Similar to the effect of composition, low interfacial slippage occurs in blends with large LCP domains, leading to less effective viscosity reduction. Thus, at 280 and 270°C, where we obtain larger VA domains, VA10 samples do not exhibit viscosity reduction, compared to the neat PTT. Furthermore, at such high temperature, PTT displays Newtonian-like behavior and thus would not be greatly affected by the presence of lubricating VA domains. As a consequence, the viscosity reduction phenomenon is observed in VA10 at temperatures of 250 and 260°C only, and is more pronounced at 250°C due to the greater interfacial area.

4.4.3 Thermal Characteristics from DSC Measurement

Table 4.2 shows the thermal data obtained from DSC scans. Both the heating traces and cooling traces are also presented in Figs. 4.11 and 4.12. The glass-transition temperature (T_g), the cold-crystallization temperature (T_{cc}), the first melting temperature (T_{mI}), and the melt-crystallization temperature (T_c) are in good agreement with those of PTT from the previous work [23], whereas the second endothermic peak temperature (T_{mII}) corresponds to the crystalline-to-nematic transition of the VA phase. The enthalpy of fusions corresponding to the first and the second endothermic peaks are denoted as $\Delta H_{m(I)}$ and $\Delta H_{m(II)}$, respectively. The transition peak of VA is very small compared to the melting peak of PTT. Even though the program is able to define the peak and even calculate the heat of fusion for blends of more than 50 wt% VA, the data cannot be exported properly. Therefore, we obtained an undulating region at around 280°C, as in Fig. 4.11. Thus, the reported $\Delta H_{m(II)}$, values will not be taken seriously.

Generally, a single T_g or its shift in blends represents miscibility or partial miscibility [24,25]. The glass transition temperature of VA was reported to be around 100°C and usually not detectable by DSC because of its low amorphous fraction [26]. In our experiments, all of the blends were immiscible at every composition, indicated by a single composition-independent T_g of the PTT phase. This value is comparable to those reported by others [26,27]. The negligible changes in T_{cc} values throughout the whole composition range might be attributed to the unchanged T_g of the blends, which indicates the unaffected molecular mobility of PTT upon crystallization from the solid, amorphous state.

The enthalpy of fusion can be used to determine the crystallization extent of a specific polymer; that is, the larger the ΔH_m is, the greater the crystallinity of the polymer. From Table 4.2, ΔH_m, without an asterisk (*) corresponds to the enthalpy of fusion not yet normalized by the weight fraction of a particular component in the blends. The subscripts (I) and (II) denote the first and second endothermic peaks, respectively. To obtain the percent crystallinity of the PTT phase (X), the enthalpy of fusion

normalized against the content of PTT in the blends, $\Delta H^{*}_{m(I)}$, must be used. The X values slightly increase at 10 wt% VA and then decrease at higher VA content. However, when the VA content does not exceed 40 wt%, $\Delta H^{*}_{m(I)}$, remains higher than that of the neat PTT, suggesting that the VA could enhance PTT crystallization ability in VA is a minor phase, and the effect is less pronounced as the VA content increases. On the contrary, if the amount of VA is not less than that of PTT, VA will hinder the PTT molecules from crystallization, resulting in smaller size and less perfection of the PTT crystallites. The higher T_c of the blends compared to the neat PTT indicates the effect of VA as a nucleating agent for PTT crystallization. In this experiment, none of the melt crystallization exotherms of the VA component could be observed [Fig. 4.12].

4.4.4 Thermogravimetric Analysis

Thermal stability of a polymeric material is one of the most important properties for both processing and application. In order to see the effect of LCP on the thermal stability of VA/PTT blends, thermogravimetric analysis was conducted. It was found that VA/PTT shows a two-step degradation. The first step corresponds to the decomposition of the PTT component, whereas the second to the VA component. Two initial decomposition temperatures, T_{d1} and T_{d2}, obtained by an extrapolation of the initial decomposition in the TGA curves, were then assigned to the onset decomposition temperatures of PTT and VA, respectively, as reported in Table 4.3. Obviously, VA exhibits a better thermal stability than PTT since it is a liquid crystalline polymer and therefore possesses excellent thermal stability due to its strong intermolecular and intramolecular forces. Increasing the amount of VA results in slightly higher T_{d1}, whereas T_{d2} remains unaffected. According to Wright's approach, the degradation temperature ($T_{d,w}$) has been defined as the temperature at which the polymer lost 1 wt% of its weight during the non-isothermal heating scan [28]. By this approach, we could observe a clearer distinction between the thermal stability of the neat polymers and the blends. Hence, it could be stated that VA/PTT blends show enhanced thermal stability.

According to Table 4.3, $T_{d,w}$ and residue content were increased with increasing amount of VA.

4.4.5 Tensile Properties

Taking into account the economic benefits, the possibility of obtaining enhanced processibility (as reported in the rheological part), and better compatibility (as seen from the smallest dispersed size), the VA10 sample was then selected for studying the temperature effect on mechanical properties. As we have found that the blend morphology is greatly affected by the fabrication temperature, it is expected that the final properties of these blends should be temperature-dependent as well. VA10 pellets were injection-molded at three different temperature profiles (see Table 4.1) and the resulting dumbbell-shaped specimens underwent the same tensile tests. The same tensile test was also performed on injection-molded PTT to observe the effects of the incorporation of a small fraction of VA on the tensile properties of the blends. According to Table 4.4, the elongation at break of all the blends exhibits a sharp decrease compared to the neat PTT, as could be expected for immiscible reinforced composites. All VA10 samples show enhanced tensile modulus but slightly-lowered tensile strength, compared to the neat PTT. This reduction in tensile strength, despite the presence of LCP, indicates poor interaction at the LCP–matrix interfaces, which is generally found in immiscible blends [13,29,30]. The open craters and holes, as well as the gaps between the dispersed VA phase and the PTT matrix observed in the tensile fractured surface [Figs. 4.13 (a)–(c)], provide clear evidence of the poor interfacial adhesion, which leads to inefficient stress transfer. An increase in tensile modulus arises from the molecular orientation and intrinsically high modulus of the VA phase.

Considering the effect of temperature on the mechanical properties of the blends, no obvious difference in tensile properties among the 10 wt% VA blends was observed, even though the maximum fabrication temperature differs by 30°C. In general, the mechanical properties of the in-situ composites strongly depend on the number of fibrils, fibril aspect ratio, and fibril orientation, including the level of molecular

orientation. A smaller viscosity ratio (in this case obtained at low temperature) should be ideal for improved mechanical performance due to the better LCP dispersion, and thus a more compatible blend is obtained. The benefits of the compatible blend are the greater contact surface area between the matrix and the dispersed size, which promotes stress transfer, and the fewer tendencies for the smaller dispersed size to induce fracture. However, apart from the good dispersion of the LCP phase in matrix, the intrinsic strength of the LCP fibrils is also critical for effective reinforcement. The neat LCP is usually processed above its rheological transition temperature (290°C) to achieve the good molecular orientation and thus stronger fibrillar structure of LCP [15]. The blends processed at higher temperature (lower shear stress provided) therefore possess a smaller fraction of spherical domains and thicker fibrils, which inherently render more strength to the material. As a result of the combined effect, it can be concluded that blends with enhanced VA dispersion obtained by lowering the fabrication temperature provide sufficient mechanical improvement similar to those with thicker fibrils. Nonetheless, the former has the advantage of easier processibility since the fine fibrillar domains lead to viscosity reduction. Further SEM analysis of the tensile fractured surfaces was consistent with rheological results [Figs. 4.13(a)–(c)]; i.e. with increasing temperature, the blend displays larger VA fibrils but inferior VA dispersion.

The tensile properties as a function of VA content, processed at 250°C, are shown in Figs. 4.14–16. Note that only blends with a low VA content of 10–40 wt% were investigated since they were fabricated at a temperature much lower than the crystalline-nematic transition of VA where the processiblity of blends with major VA content could be intricate. The percent elongation at break obviously decreases by the incorporation of VA, as expected for typical short-fiber reinforced composites (see Fig. 4.14). The elongation at break is drastically dropped by introducing 10 wt% VA and then is slightly affected by the further increasing of VA content. As depicted in Fig. 4.15, the tensile strength of the blends continually decreases with increasing VA content. Blends with higher VA content clearly exhibited inferior tensile strength as a result of ineffective stress transfer from the PTT matrix to the large VA domains. Hence, the

effects of VA domain size on the tensile properties are more obvious with regards to VA content than to temperature. As shown in Fig. 4.16, the Young's modulus markedly improves with increasing VA content, as expected. For the blend with 40 wt% VA, the increase in the modulus is about 1.3-fold from 854 to 1117 MPa compared to the neat PTT.

4.5 Conclusions

In this work, Vectra A950 (VA), poly(trimethylene terephthalate) (PTT), and their blends were subjected to different flow conditions in a capillary rheometer. The rheological, morphological, thermal, and mechanical properties of the blends were investigated. Study of the high-viscosity-ratio system of the binary blends of PTT/VA by rheological approach revealed that VA exhibited stronger shear-thinning behavior but less temperature sensitivity, compared to PTT. The incorporation of VA into PTT led to enhanced shear-thinning and greater temperature sensitivity; the latter was reflected in the increase in the flow activation energies of the blends with increasing VA. From SEM analysis, increasing temperature and VA content tended to enlarge the VA domain size, thus decreasing the interfacial area between PTT and VA. High shear stress (obtained at low extrusion temperature or high shear rate), as well as low VA content, was required to obtain viscosity reduction due to the increased interfacial area between each component. From the tensile tests, it was found that introducing 10 wt% VA enhanced the tensile modulus, slightly decreased the tensile strength, and drastically dropped the elongation at break. Moreover, it showed sufficiently improved tensile properties, similar to those fabricated at higher temperatures. However, more pronounced effects of the larger VA domain size on the inferiority of mechanical performance were observed with respect to changes in VA content.

Thermal property results indicated that the blends were immiscible as the glass transition temperature and the melting temperature remained unchanged throughout the entire composition. VA increased the melt crystallization temperature of the PTT phase

as a result of the nucleation effect but did not significantly influence the cold crystallization process, regardless of the VA content. The incorporation of VA also provided blends with improved thermal stability, according to Wright's approach.

4.6 Acknowledgements

The authors are grateful to the Royal Golden Jubilee Ph.D. Program.

4.7 References

[1] M.T. Heino, J.V. Seppala, Polym. Bull. 30 (1993) 353-360.

[2] B. Liang, L. Pan, X. He, J. Appl. Polym. Sci. 66 (1997) 217-224.

[3] G.P. Chang-Chien, M.M. Denn, Polym. Adv. Technol. 7 (1996) 168-172.

[4] F.P. La Mantia, A. Valenza, M. Paci, P.L. Magagnini, Rheol. Acta. 28 (1989) 417-422.

[5] P.J. Flory, Macromolecules 11 (1978) 1138-1141.

[6] G. Kiss, Polym. Eng. Sci. 27 (1987) 410-423.

[7] J.S. He, W.S. Bu, Polymer 35 (1994) 5061-5066.

[8] A.R. Postema, P.J. Fennis, Polymer 38 (1997) 5557-5564.

[9] D. Beery, S. Kenig, A. Siegmann, Polym. Eng. Sci. 31 (1991) 451-458.

[10] G. I. Taylor, Proceedings of the Royal Society A 138 (1932) 41-48.

[11] G. I. Taylor, Proceedings of the Royal Society A 146 (1934) 501-523.

[12] S. Bastida, J.I. Eguiazabal, J. Nazabal, J. Mater. Science 35 (2000) 153-158.

[13] A.K. Kalkar, A.A. Deshpande, M.J. Kulkarni, J. Appl. Polym. Sci. 106 (2007) 34-

45.

[14] L.P. Tan, C.Y. Yue, K.C. Tam, Y.C. Lam, X. Hu, Polym. Int. 51 (2002) 398-405.

[15] L.E. Nielsen, Polymer Rheology, Marcel Dekker, New York, (1977) p47.

[16] C. Crevecoeur, G. Groeninckx, J. Appl. Polym. Sci. 49 (1993) 839-849.

[17] Y.Z. Meng, S.C. Tjong, Polymer 39 (1998) 99-107.

[18] V.G. Kulichikhin, O.V. Vasileva, I.A. Litvinov, E.M. Antipov, I.L. Parsanyan, N.A. Plate, J. Appl. Polym. Sci. 42 (1991) 363-372.

[19] J. He, W. Bu, H. Zhang, Polym. Eng. Sci. 35 (1995) 1695-1074.

[20] H.J. Eyring, J. Chem. Phys. 4 (1936) 283-291.

[21] S. Saengsuwan, S. Bualek-Limcharoen, G.R. Mitchell, R.h. Olley, Polymer 44 (2003) 3407-3415.

[22] M. Pyda, A. Boller, J. Grebowicz, H. Chuah, B.V. Lebedev, B.j. Wunderlich, Polym. Sci. Part B Polym. Phys. 36 (1998) 2499-2511.

[23] N. Dangseeyun, P. Supaphol, M. Nithitanakul, Polym. Test. 23 (2004) 187-194.

[24] J.C. Ho, T.C. Lin, K.H. Wei, Polymer 41 (2000) 9299-9304.

[25] P. Xing, X. Ai, L. Dong, Z. Feng, Macromolecules 31 (1998) 6898-6907.

[26] P. Krutphun, P. Supaphol, Eur. Polym. J. 41 (2005) 1561-1568.

[27] M.T. Run, Y.J. Wang, C.G. Yao, H.C. Zhao, J. Appl. Polym. Sci. 103 (2007) 3316-3325.

[28] J. Wright, Thermal degradation of polymers. Soc. Chem. Industries 13 (3) (1961)

p. 248.

[29] A.A. Handlos, D.G. Baird, JMS Rev. Macromol. Chem. Phys. C35(2) (1995) 183-238.

[30] L.E. Nielsen, Mechanical properties of polymers and composites II; Marcel Dekker: New York, 1974.

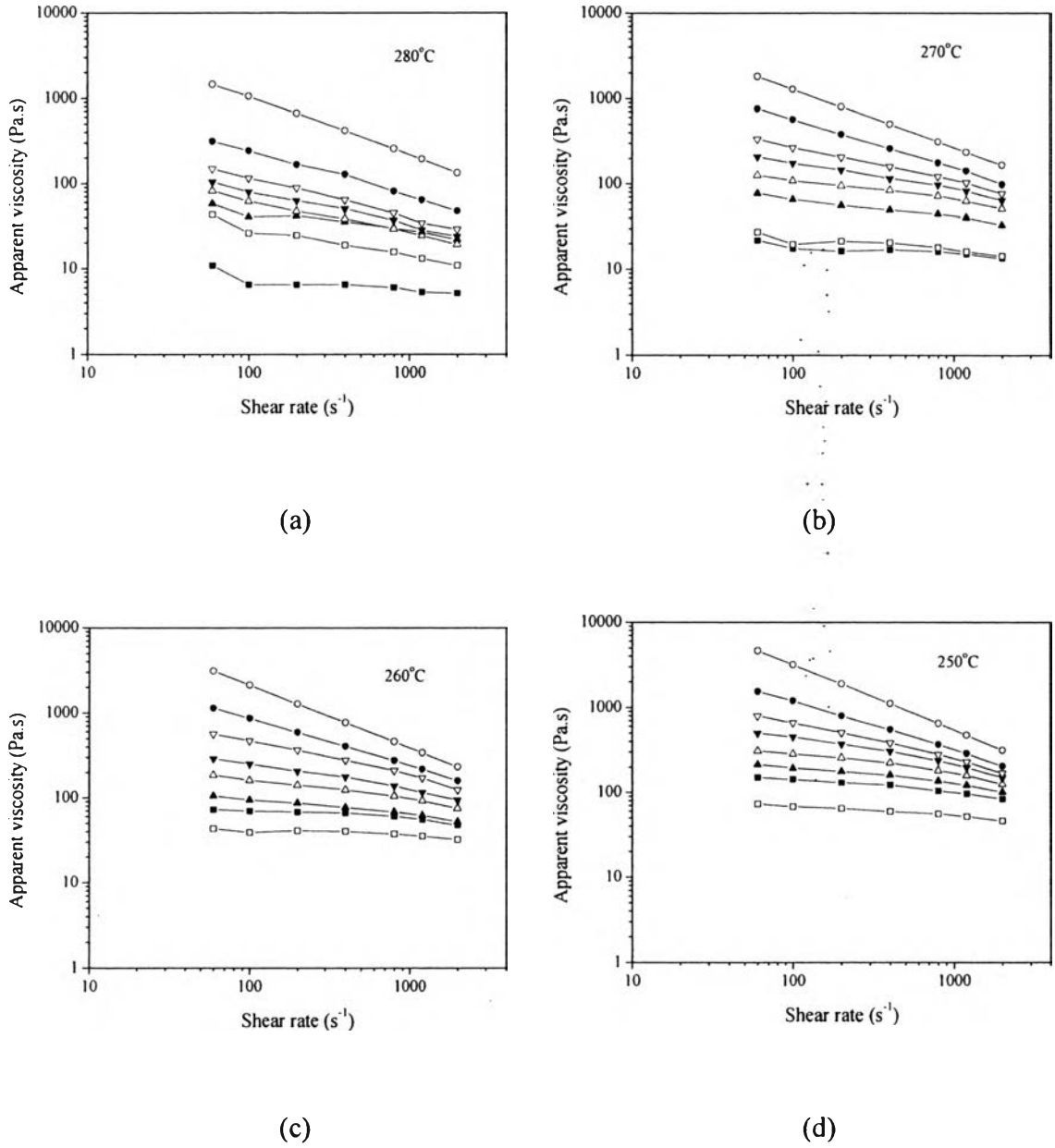

Figure 4.1 Rheological curves of PTT, VA and their blends containing various VA contents of (■) 0, (□) 10, (▲) 20, (△) 30, (▼) 40, (▽) 50, (●) 70, and (○) 100 wt% using a 1-mm diameter capillary with an L/D of 20 measured at (a) 280°C, (b) 270°C, (c) 260°C, and (d) 250°C.

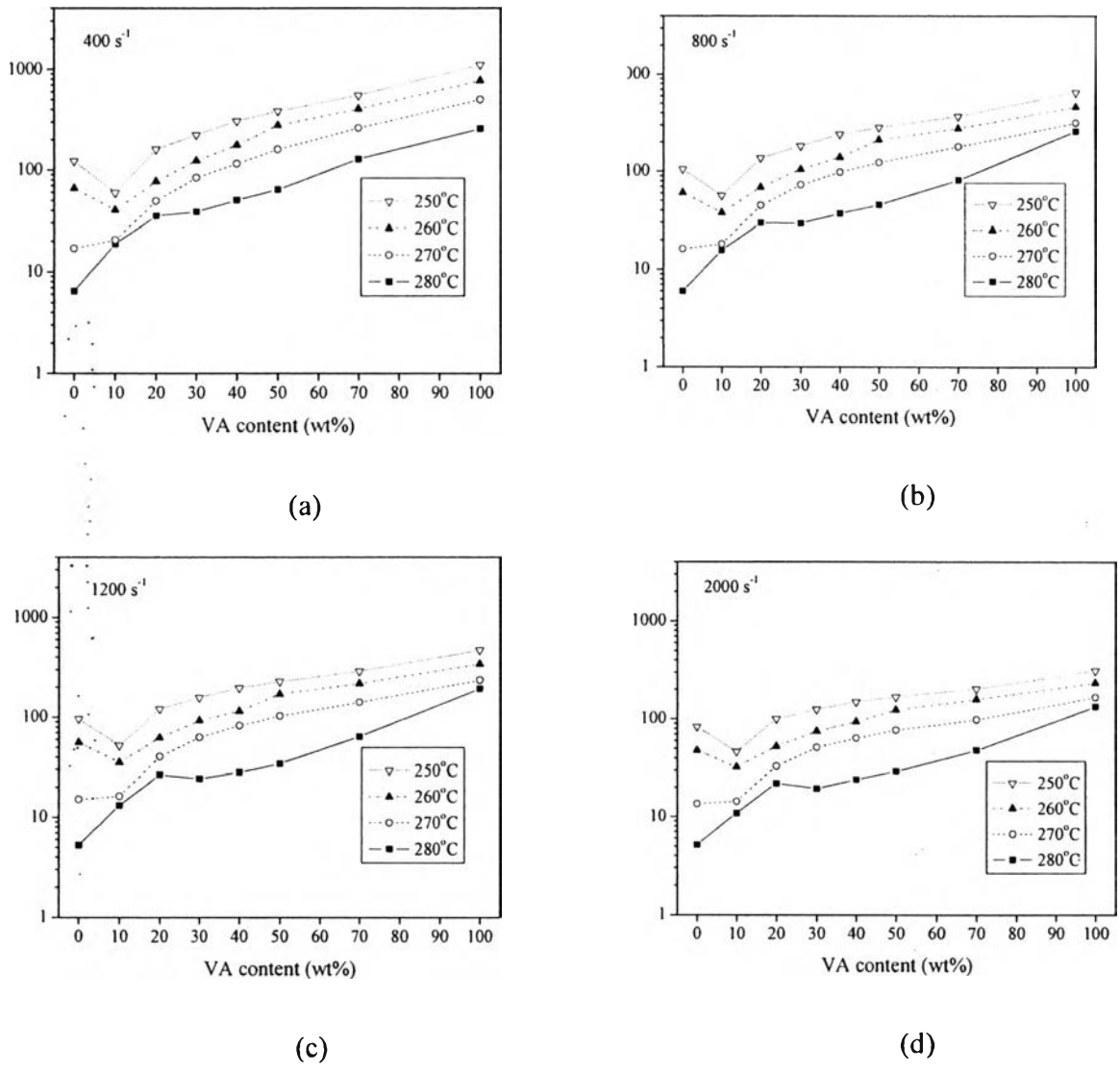

Figure 4.2 Plots of compositional dependence of shear viscosity of PTT, VA, and their blends extruded at various temperatures and a shear rate of (a) 400 s^{-1}, (b) 800 s^{-1}, (c) 1200 s^{-1}, and (d) 2000 s^{-1}.

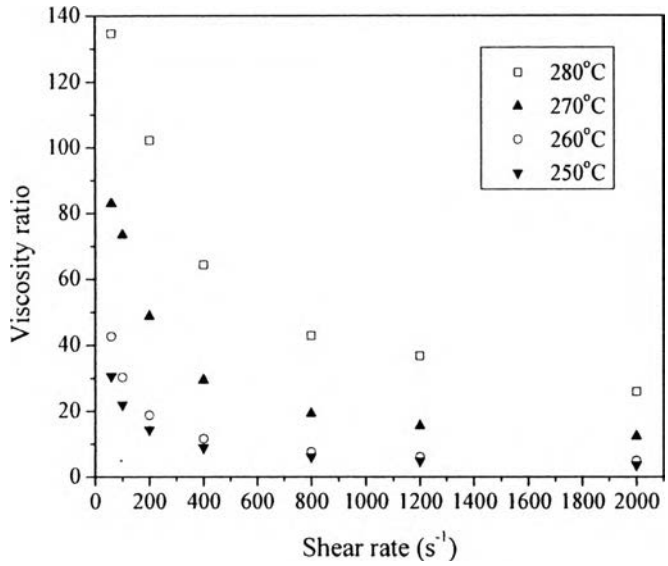

Figure 4.3 VA/PTT viscosity ratios as a function of shear rate for various temperatures.

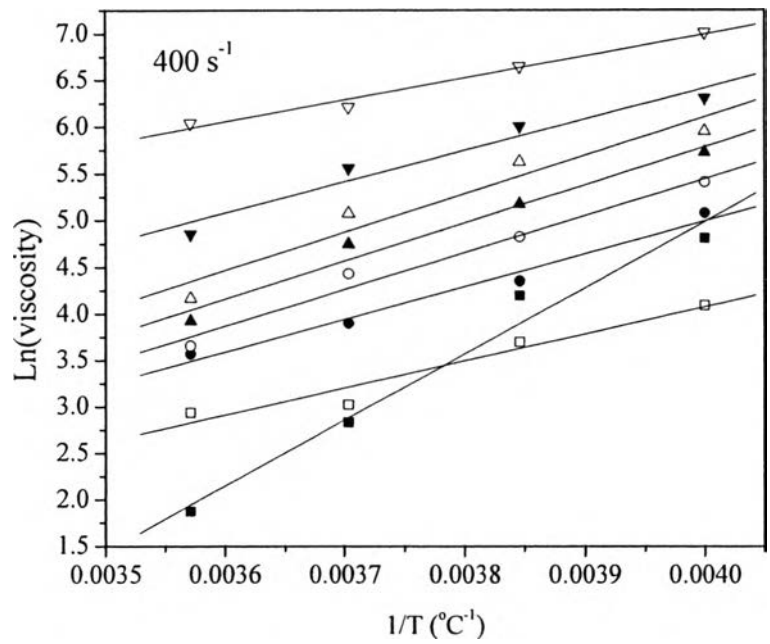

Figure 4.4 Plots of $\ln\eta_a$ vs. 1/T for PTT and VA extrudates with VA contents of (■) 0, (□) 10, (●) 20, (○) 30, (▲) 40, (△) 50, (▼) 70, (▽) 100 wt% at a shear rate of $400s^{-1}$.

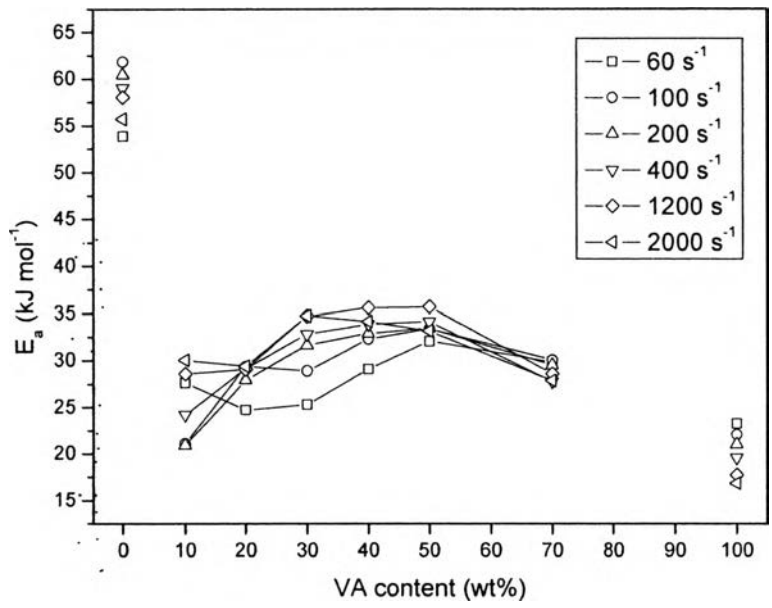

Figure 4.5 Plots of compositional dependence of flow activation energy of PTT, VA, and their blends extruded at various shear rates.

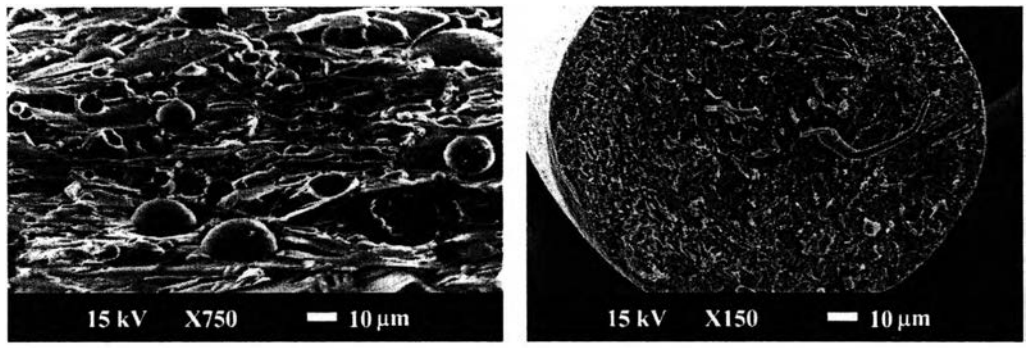

Figure 4.6 Scanning electron micrographs of VA/PTT blends showing (a) the fractured surface of the twin-screw extrudate, and (b) the fractured surface of the 20 wt% VA rheometer extrudate after shearing at 2000 s^{-1}, 260°C.

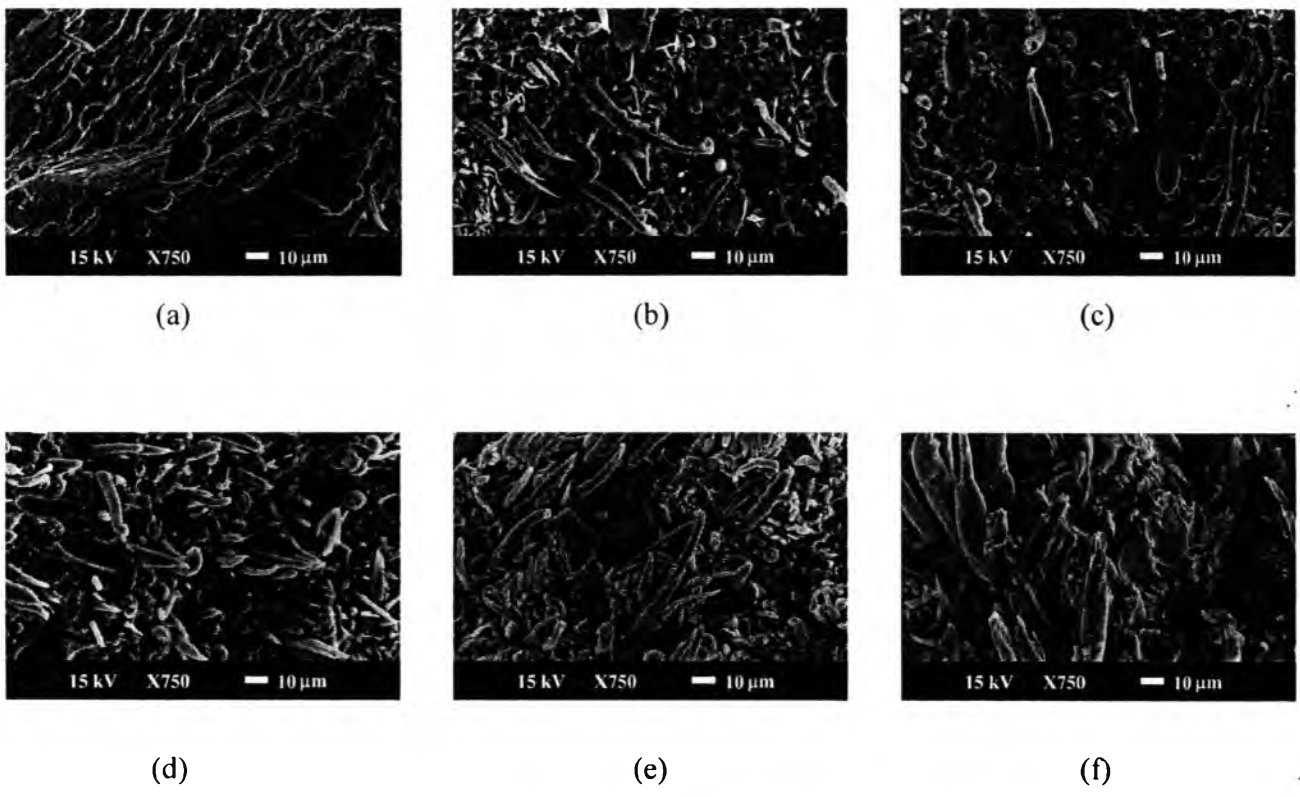

Figure 4.7 Scanning electron micrographs of VA/PTT strands extruded through a capillary with a constant strain rate of 2000 s^{-1}, temperature 260°C, and VA contents of (a) 10, (b) 20, (c) 30, (d) 40, (e) 50, and (f) 70 wt%.

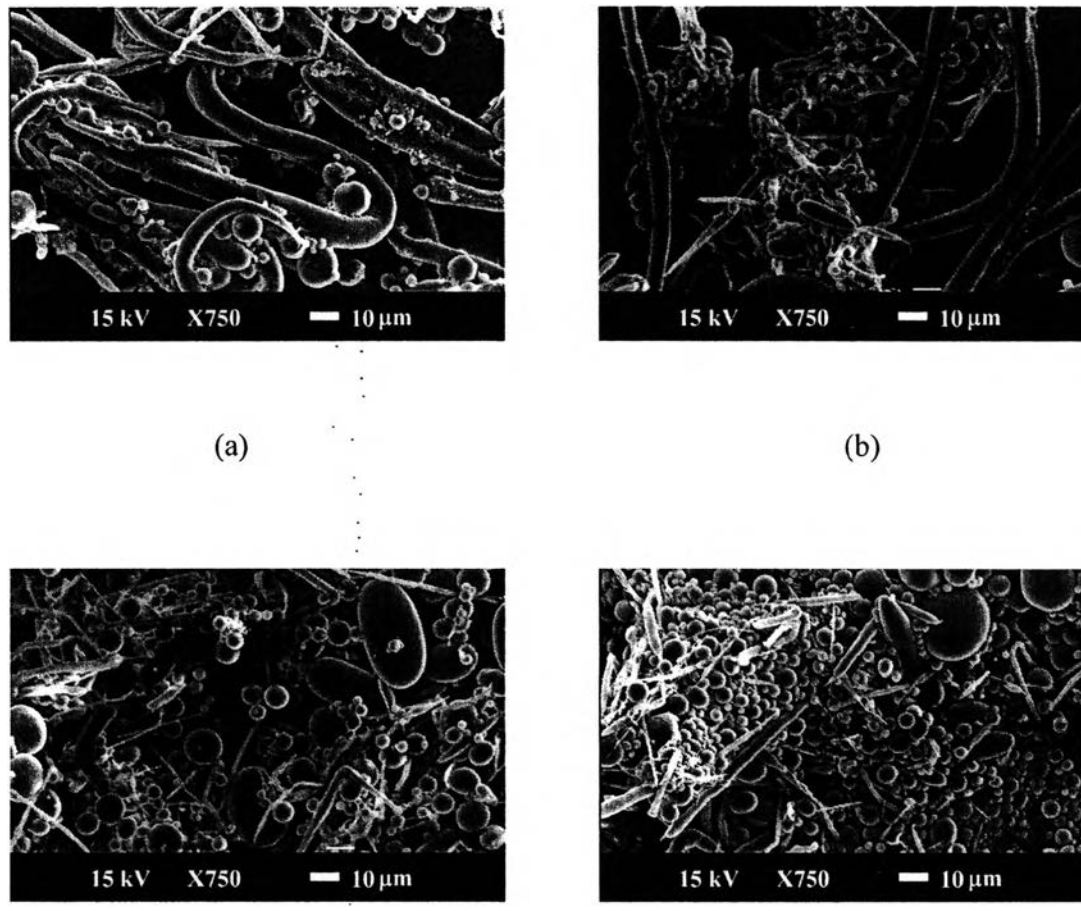

Figure 4.8 Scanning electron micrographs of residues extracted from the blends of VA/PTT with a VA content of 10 wt%, extruded through a capillary at a shear rate of 2000 s^{-1} and temperature of (a) 280°C, (b) 270°C, (c) 260°C, and (d) 250°C.

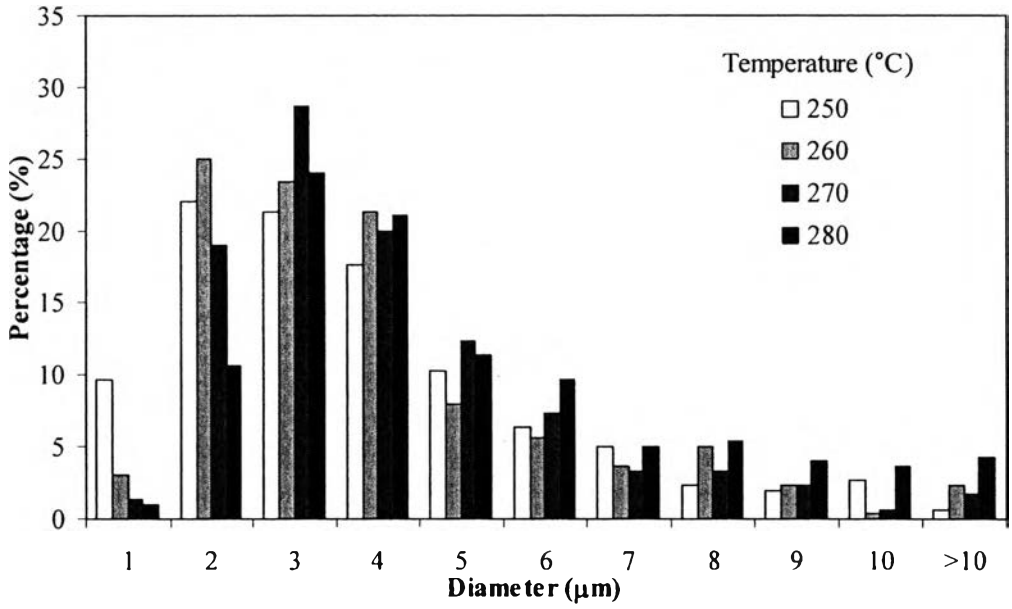

Figure 4.9 Diameter distribution of the VA residue in the rheometer extrudates at a shear rate of 2000 s^{-1} and various temperatures.

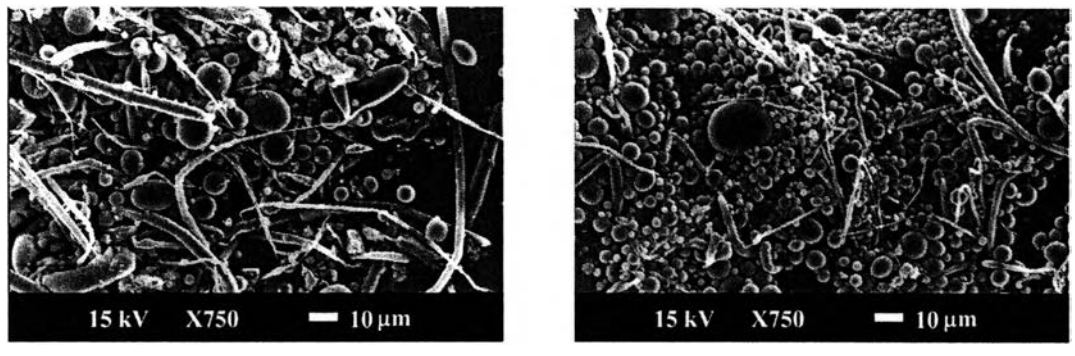

(a) (b)

Figure 4.10 Scanning electron micrographs of residues extracted from the blends of VA/PTT with a VA content of 10 wt%, extruded through a capillary at temperature 250°C, and shear rate of (a) 400 s^{-1}, and (b) 2000 s^{-1}.

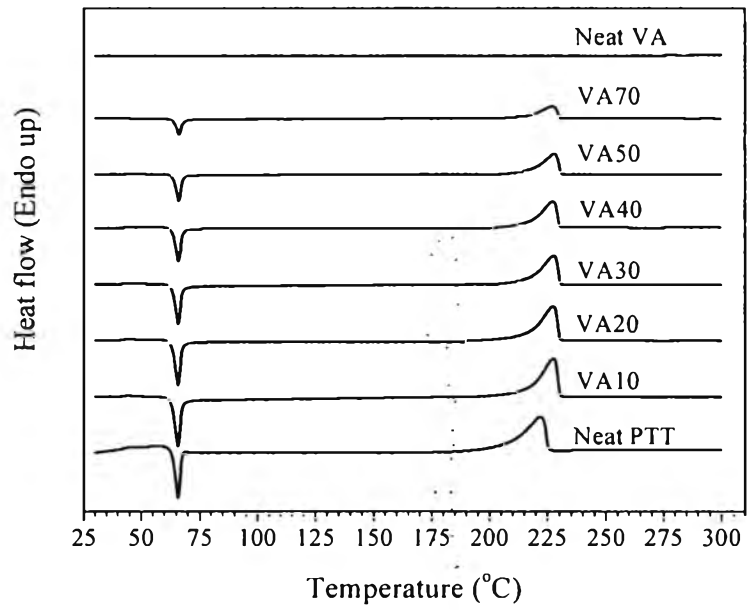

Figure 4.11 DSC second heating traces of the neat VA, PTT, and their blends after melt-annealing at 300°C for 5 min and quenching in liquid N_2 for 10 min. The heating rate is 5°C/min.

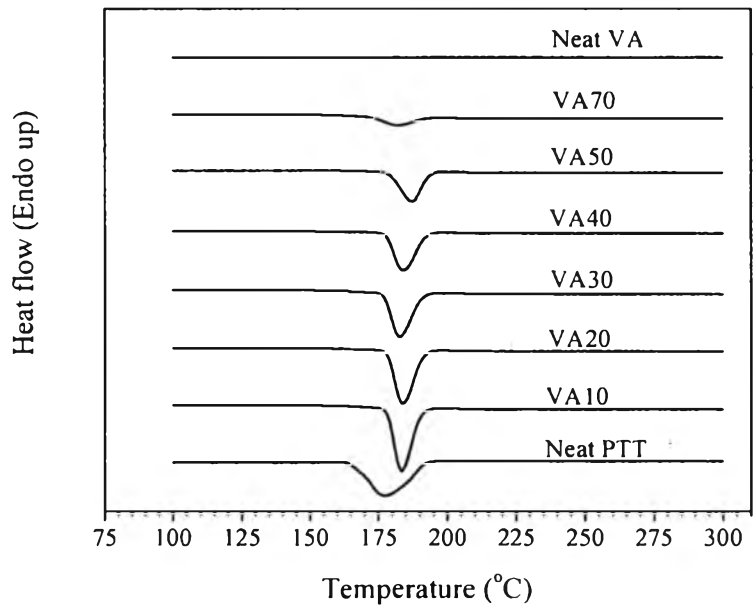

Figure 4.12 DSC cooling traces of the neat VA, PTT, and their blends. The cooling rate is 10°C/min.

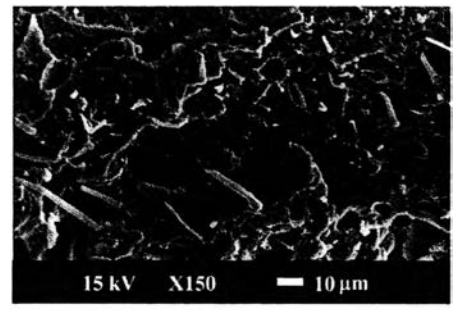

(a)

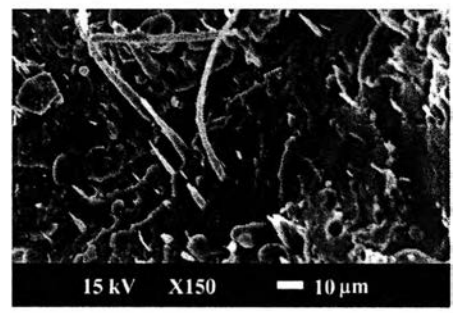

(b)

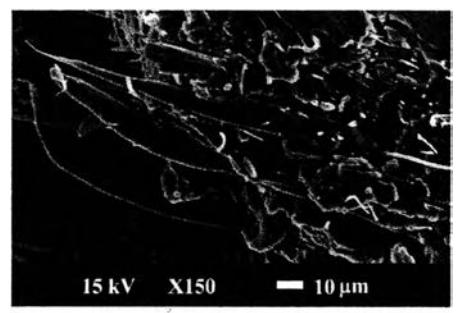

(c)

Figure 4.13 Scanning electron micrographs of the tensile fractured surfaces of (a) VA10-250, (b) VA10-265, and (c) VA10-280.

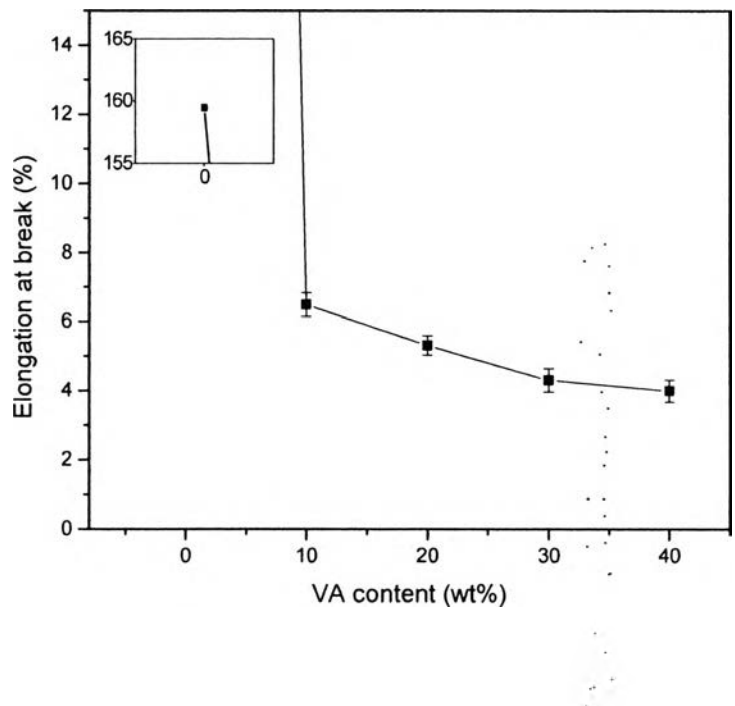

Figure 4.14 Elongation at break of injection-molded PTT and PTT/VA blends processed at 250°C.

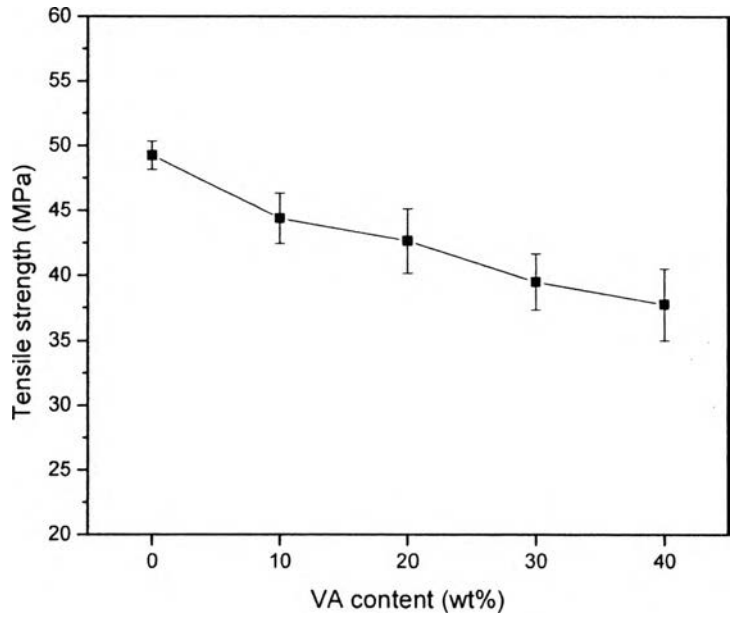

Figure 4.15 Tensile strength of injection-molded PTT and PTT/VA blends processed at 250°C.

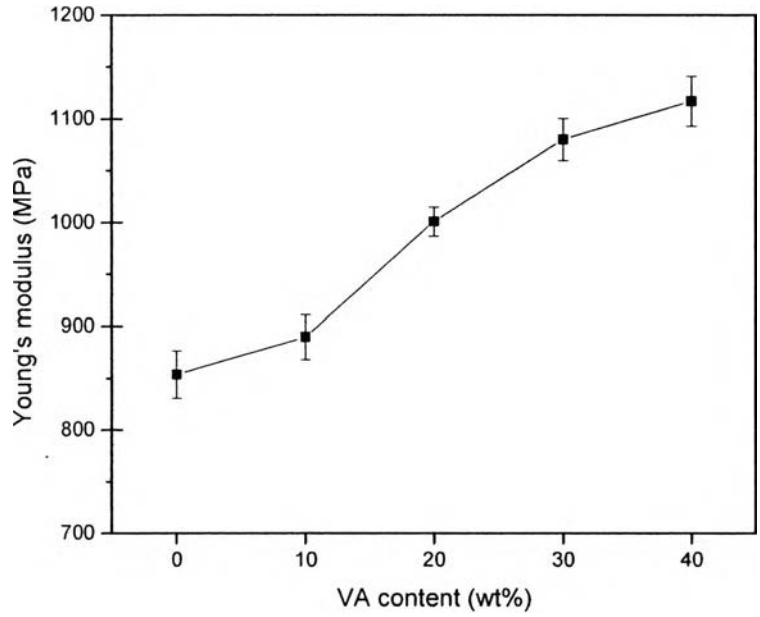

Figure 4.16 Tensile modulus of injection-molded PTT and PTT/VA blends processed at 250°C.

Table 4.1 Injection molding conditions for the neat PTT, VA, and their blends

Sample	Temperature (°C)						Injection time (s)	Cooling time (s)
	Zone 1	Zone 2	Zone 3	Zone 4	Nozzle	Mold		
PTT	220	230	240	250	220	90	3	30
VA10-250	220	230	240	250	220	90	3	30
VA10-265	235	245	255	265	220	90	3	35
VA10-280	250	260	270	280	220	90	3	40
VA20	220	230	240	250	220	90	3	30
VA30	220	230	240	250	220	90	3	30
VA40	220	230	240	250	220	90	3	30

Table 4.2 DSC characteristics of VA, PTT, and their blends

VA wt%	T_g (°C)	T_{cc} (°C)	T_{mI} (°C)	$\Delta H_{m(I)}$ (J/g)	$\Delta H^*_{m(I)}$ (J/g)[b]	(X) (%)[a]	T_{mII} (°C)	$\Delta H_{m(II)}$ (J/g)	$\Delta H^*_{m(II)}$ (J/g)[c]	T_c (°C)
100	-	-	-	-	-	-	279.15	0.99	0.99	-
70	-	66.10	227.13	18.39	61.30	42.10	281.61	0.58	0.83	182.01
50	41.22	65.98	227.90	33.42	66.84	45.91	282.09	0.29	0.58	187.16
40	42.13	65.91	227.33	41.38	68.97	47.37	-	-	-	184.24
30	42.60	65.76	227.61	47.86	68.37	46.96	-	-	-	182.95
20	42.02	65.69	227.50	56.07	70.09	48.14	-	-	-	184.00
10	42.94	65.70	227.52	64.24	71.38	49.02	-	-	-	183.52
0	42.60	65.73	227.55	68.74	68.74	47.21	-	-	-	174.10

[a] The percent crystallinity (χ) of the PTT component was calculated assuming a heat of fusion of PTT crystals of 145.6 J/g [22].

[b] Heat flow was normalized against the weight fraction of the PTT component.

[c] Heat flow was normalized against the weight fraction of the VA component.

Table 4.3 TGA results of VA, PTT, and their blends

Composition (VA/PTT)	T_{d1} (°C)	T_{d2} (°C)	$T_{d,w}$ (°C)	Residue at 700°C (%)
100/0	-	500.0	446.9	49.1
70/30	381.0	500.1	367.5	36.0
50/50	375.1	499.9	359.3	27.7
40/60	376.6	500.6	357.8	24.2
30/70	375.7	507.2	356.9	22.0
20/80	376.3	500.0	353.9	19.3
10/90	376.2	499.8	347.9	12.5
0/100	375.8	-	330.6	4.7

Table 4.4 Mechanical properties of injection-molded PTT and VA10 processed at different temperature profiles

Mechanical property	Sample			
	PTT	VA10-250	VA10-265	VA10-280
Elongation at break (%)	159.48±8.3	6.49±0.4	6.45±0.5	6.85±0.7
Tensile strength (MPa)	49.24±1.1	44.38±1.9	42.95±0.6	45.60±2.4
Young's modulus (MPa)	727.88±22.8	889.57±21.6	853.57±31.2	876.52±21.5